JOURNAL OF AGRICULTURAL AND FOOD CHEMISTRY

Article

pubs.acs.org/JAFC

# Effect of Water Migration between Arabinoxylans and Gluten on Baking Quality of Whole Wheat Bread Detected by Magnetic Resonance Imaging (MRI)

Juan Li,[†] Ji Kang,[†] Li Wang,[†] Zhen Li,[†] Ren Wang,[†] Zheng Xing Chen,*[,†] and Gary G. Hou*[,§]

[†]School of Food Science and Technology, State Key Laboratory of Food Science and Technology, Jiangnan University, Wuxi, Jiangsu 214122, People's Republic of China

[§]Wheat Marketing Center, 1200 N.W. Naito Parkway, Suite 230, Portland, Oregon 97209, United States

**ABSTRACT:** A new method, a magnetic resonance imaging (MRI) technique characterized by $T_2$ relaxation time, was developed to study the water migration mechanism between arabinoxylan (AX) gels and gluten matrix in a whole wheat dough (WWD) system prepared from whole wheat flour (WWF) of different particle sizes. The water sequestration of AX gels in wheat bran was verified by the bran fortification test. The evaluations of baking quality of whole wheat bread (WWB) made from WWF with different particle sizes were performed by using SEM, FT-IR, and RP-HPLC techniques. Results showed that the WWB made from WWF of average particle size of 96.99 $\mu$m had better baking quality than those of the breads made from WWF of two other particle sizes, 50.21 and 235.40 $\mu$m. $T_2$ relaxation time testing indicated that the decreased particle size of WWF increased the water absorption of AX gels, which led to water migration from the gluten network to the AX gels and resulted in inferior baking quality of WWB.

**KEYWORDS:** *magnetic resonance imaging (MRI), arabinoxylan (AX), gluten, water migration, whole wheat bread*

## INTRODUCTION

Whole wheat bread (WWB) is one of the fastest-growing staple foods in Western countries.[1] Many scientific studies have confirmed its antioxidative activity and other nutritional functions in epidemiology.[2−5] However, due to the less cohesive (also water partitioning during mixing and baking) property of whole wheat dough (WWD) compared with that of white dough, the baking qualities of WWB, including loaf volume, specific volume, and interior structure (the porosity of bread), are inferior to those of white bread,[6] which has restricted a wider acceptance of WWB by consumers.[7] In Asian countries, there are many fewer whole wheat products and a lower market shares, leading to increased incidence rates of chronic diseases and reduced value of grains (more grain components go to feed).[8]

The relationship between the particle size of wheat bran and the volume of bread has been investigated, but the results were inconclusive and controversial. Some studies have shown that the wheat bran has a negative effect on bread volume,[9,10] especially small bran particles.[11,12] Wheat bran particles can deleteriously affect the gluten network, decrease dough resilience, and impair the framework of gas cells and, thus, gas retention. These effects can lead to low bread specific volume and inferior baking quality.[13] However, other research has shown that bread made from smaller bran particle size flour had a larger volume than bread made with coarser bran flour.[14] Meanwhile, there were some results suggesting that bread with the medium particle size (415 $\mu$m) of wheat bran had larger volume than either the refined (278 $\mu$m) or the coarse group (609 $\mu$m).[9] More studies are still needed to investigate the effect of whole wheat flour (WWF) particle size on its baking quality.

Arabinoxylans (AX) are important nonstarch polysaccharides that form the cell walls of cereal endosperm and bran.[15] Ferulic acid (FA) is a major phenolic acid in wheat, where it is mainly esterified to the arabinose backbone of AX.[16,17] In wheat bran, it is concentrated in cell walls. Incorporation of ferulic acid into arabinose residues enhances the formation of intermolecular cross-links of AX, leading to gel formation.[18] Previous research reported that the AX gels can inhibit the formation of gluten network by changing water distribution among gluten and other macromolecules and result in a less extensible gluten.[19] This is especially true when AX gels compete with the gluten network for water during mixing, restraining the gluten network from water uptake.[20] Gill[21] proposed the redistribution of water from nonstarch polysaccharides to gluten during fermentation. Jacobs[7] theorized that AX tightly binds water in the dough system, reducing the availability of water for developing the gluten network. Roman-Gutierrez et al.[22] compared the water vapor adsorption properties of wheat flour and flour components (pentosans, gluten, and starch) using a controlled atmosphere microbalance, and the theoretical distribution of water between the flour components was determined under a water vapor environment. Roman-Gutierrez et al. demonstrated that the water vapor adsorption properties of wheat flour depended only on the ability of the flour components to interact directly with the water molecules, which may not apply to the bread dough system that traps a large amount of water

Received: March 19, 2012
Revised: June 13, 2012
Accepted: June 15, 2012
Published: June 15, 2012

inside macromolecular complexes formed by the swollen components.

The magnetic resonance imaging (MRI) technique is a tool for the noninvasive determination of moisture distribution in high-moisture samples, including grain kernels.[23] Traditionally, MRI was applied to examine macro-water distribution and migration in grain, such as water migration in single rice kernels during the tempering process,[24] water penetration into rice grains during soaking,[25] and water redistribution in grain kernels during drying.[26] Moreover, MRI techniques have been developed to show the internal structure of bread, which can simplify the complicated and time-consuming process of sensory and visual instrumental evaluation and reduce costs.[27,28] MRI has been considered to be an accurate and nondestructive method for visualizing the internal network structure of bread[29] and calculating the porosity of air cells.[30−32]

The present work was undertaken to evaluate the effect of WWF particle size on bread-baking performances that were characterized by loaf volume and crumb porosity. To gain more insight into relationships between particle size and bread quality, a MRI technique was applied to examine the water migration between macromolecules (AX gels and gluten). To the best of our knowledge, despite the plenitude of hypotheses that have been proposed concerning water migration and competitive water absorption between AX gels and the gluten network, no definitive evidence has been presented to support these mechanisms. The present study's goal was to verify the water migration pattern and competitive water absorption mechanism between AX gels and gluten through the MRI technique and to confirm that it was the mechanism of inferior loaf volume of WWB caused by refined particle size flour.

## MATERIALS AND METHODS

**Wheat Grain.** Wheat grain (Zheng 9023 cultivar, harvested in 2008) was obtained from Jin Lenong Agriculture Development Co., Ltd. (Henan Province, China).

**WWF Analysis.** Ash content (12% moisture basis) was 1.60% and protein content (12% moisture basis, N × 5.7) was 13.0%, as reported by the supplier. Farinograph curves were obtained according to AACC International Approved Method 54-21.

**Chemicals.** Bakery sugar, salt, shortening, and instant dry yeast were purchased from a local supermarket. The chemicals used for preparing scanning electron microscopy (SEM) samples and testing the content of FA were of analytical grade and purchased from Sinopharm Chemical Regent Co. (Shanghai, China).

**WWF Milling.** The WWF was milled from intact wheat kernel samples using a Waring blender (DFY-400, Wenling Dade Traditional Chinese Medicine Machinery Co., Ltd., Zhejiang Province, China) by grinding for 5 min. The coarse flour was superfine ground by the ultramicro pulverizer (MZF-4, Hengtai Dongqi Powder and Equipment Co., Ltd., China) for 15, 25, and 35 min, respectively to achieve the desired particle sizes. Four hundred grams WWF of each particle size group was prepared each time. All experiments were repeated three times.

**Particle Size Analysis.** The particle size distributions of WWF obtained from different milling times were measured by the Laser Particle Size Analyzer (S3500, Microtrac Inc., USA), and the measurements were triplicates. The data were fitted by Origin (version 8.5), and the average particle size was obtained from the fitted curve.

**Breadmaking.** Bread loaves (each made from 150 g of dough) were made in duplicate using AACC Approved Method 10-10B (optimized straight-dough; AACC International, 2000) with some adjustments. Formulation was as follows: WWF, 500 g; sugar, 30 g; salt, 7.5 g; shortening, 15 g; and instant dry yeast, 15 g. Control bread was prepared from a commercial white bread flour (China Oil and Foodstuffs Corp., Qinhuangdao, Hebei, China). Commercial bread flour quality parameters were as follows: ash content, 0.40% (14% mb) and protein content, 14.0% (14% mb). Yeast was dissolved in water containing 0.1% sugar at 30 °C before use. Optimum absorption of 68% was acquired from the Farinogram data (11.3% mb). Dough was mixed in a bread mixer (hook-mixer with a 1 kg mixing bowl; Guangzhou Chenggong Baking Machinery Co., Ltd. China). Ingredients were mixed at speed 2 for 5−8 min (optimized in preliminary assays). Then the dough was divided into 150 g per piece, placed into a rectangular baking pan (10 × 5 × 3 cm), and fermented at 27 °C for 30 min, which was adjusted from the 90 min adopted in AACC International Approved Method 10-10B (2000) to avoid dough collapse after a long fermentation time. Then, the dough was punched down and proofed for 90 min (increased from 33 min, because this was found to greatly improve the volume of WWB) at 38 °C with 85% relative humidity in a proofing cabinet. Baking was conducted in an oven (HXM-CS11-10, Shanghai Qingyou Industrial Co., Ltd., China) for 25 min at 170 °C upper temperature and 210 °C bottom temperature. After cooling for 1 h, bread samples were placed into plastic bags and stored in a freezer at −18 °C until analyses. Bread slices (1.0 cm) were cut by an electronic bread cutter for MRI analysis.

**Evaluation of Bread Quality.** *Determination of Bread Specific Volume.* After cooling for 1 h at room temperature on metal grids, the bread weight and volume were measured in triplicates. Bread volume was determined by the rapeseed displacement method (AACC International Approved Method 10-05). The specific volume ($cm^3\ g^{-1}$) of bread was calculated by dividing the volume by the weight.

*Calculation of the Bread Porosity from MR Images.* The crumb structure of the WWB slices was evaluated for porosity, as observed with an MRI system (Mini MR-60, Shanghai Niumag Electronics Technology Co., Ltd., Shanghai, China). Image analysis was performed by the spin−echo 2D-FT method using an echo time of 0.1 ms and a repetition time of 0.5 s according to the testing parameters provided by the instrument manufacturer (Shanghai Niumag Electronics Technology Co. Ltd.). The images were recreated on a 192 × 192 matrix for 2D images, which were scanned for three layers with a 4.9 mm thickness of each layer. The porosity was calculated by the image twice-threshold segmentation method[33] using Matlab (version R2010a) to offset the variation error caused by the signal-to-noise ratio of the scanned images. The gray value range of image was 0−255. The contrast of the images was adjusted and selected from the gray value for detecting the rim of the bread sample; the pixel amount of bread sample was designated $N_1$. The threshold value was adjusted and selected again for testing the internal gas cell of the bread; the pixels lower than the threshold were counted and designated $N_2$, representing the gas cells of the bread crumb. Therefore, the pixels that were higher than the threshold represented the backbone structure of the bread. The porosity can be calculated from eq 1 provided by the instrument manufacturer (Shanghai Niumag Electronics Technology Co. Ltd.). $N$ is the number of pixels, $S_{pixel}$ is the physical area of a single pixel, and $h$ is the thickness of a bread cross section. $V_{pore}$ is the total volume of the gas cells, and $V_{total}$ is the total volume of the bread, including the gas cell volume and the volume of bread crumb.

$$\varnothing_{MRI} = \frac{V_{pore}}{V_{total}} \times 100\% = \frac{N_2 S_{pixel} h}{N_1 S_{pixel} h} \times 100\% = \frac{N_2}{N_1} \times 100\% \quad (1)$$

**Evaluation of Effect of WWF Particle Size on Bread-Baking Quality.** *SEM.* The interaction between the wheat bran and gluten matrix was observed by scanning electron microscope (Quanta-200, FEI Co., Ltd., USA). The WWD (dough samples were taken after they were properly mixed during the bread-baking process) was fixed with aqueous 3.0% (v/v) glutaraldehyde for 72 h and washed six times with 0.1 M sodium phosphate buffer (pH 7.2) followed by aqueous 1.0% (w/v) $OsO_4$ for 2 h at 4 °C. Samples were then rinsed for 1 h in distilled water and dehydrated in a graded acetone series in five steps. After drying with a critical point dryer, the samples were mounted on

bronze stubs and sputter-coated with gold (50 Å thick). Then specimens were observed and photographed with an accelerating voltage of 5.0 kV and viewed at magnification levels of 1200×.

*Fourier Transform Infrared Spectroscopy (FT-IR).* Three doughs (100 g/each) were produced by mixing three different particle sizes of WWF with 68% $D_2O$ (w/w) (for deducting the background of the pure water) for 3 min using the same bread mixer as described previously. The secondary structure of gluten protein in WWD was determined in triplicates by FT-IR (NEXUS, Nicolet Co., Ltd., USA). The data were processed by Omnic and Peak Fit software (version 4.12).[34]

**Determination of FA Content by Reversed Phase High-Performance Liquid Chromatography (RP-HPLC).** *Extraction of FA from WWF.* WWF (2 g) and distilled water (11.3 g) were weighed into a 250 mL shake flask, and the mass fraction of WWF was 15% (w/w). Thermostable $\alpha$-amylase (0.002 g; 30 U/mg, Novozyme, Denmark) was added. The starch component in WWF was hydrolyzed in ab 84 °C thermostatic water bath for 40 min. The $\alpha$-amylase was inactivated in a 100 °C boiling water bath for 10 min. After the samples were hydrolyzed, alkali protease (0.001 g, 100 U/mg, Novozyme) was added to the solution, the pH value was adjusted to 8.0 with sodium hydroxide (1.5% w/v), and the mixture was shaken in a water bath (55 °C) for 120 min. After hydrolysis by alkali protease, the enzyme was inactivated by a 100 °C boiling water bath for 10 min. Glucoamylase (0.5 mg; 100 U/mg, Novozyme) was added, and the pH of the solution was adjusted to 4.5 with 2 mol/L hydrochloric acid. The samples were shaken in a water bath (60 °C) for 120 min, after which the glucoamylase was inactivated in a boiling water bath for 10 min. The suspension was centrifuged at 4 °C for 15 min at 5000 rpm, and the residue was decanted into another 250 mL shake flask. Finally, 150 mL of sodium hydroxide (1.5% w/v) was added for alkali hydrolyzation in a water bath (85 °C) for 2 h. The suspension was centrifuged for 15 min at 8000 rpm. The pH of the supernatant (5 mL) was adjusted to 2.5 with 2 mol/L hydrochloric acid. The FA was extracted by 10 mL of diethyl ether for 5 min, and the diethyl ether was evaporated using a rotary evaporator (RV 10 basic, IKA, Germany) at 45 °C. The FA extract was dissolved by 2 mL of methanol. All of the experiments were conducted in three replicates.

*RP-HPLC Analysis of FA.* The FA extract was identified and quantified in triplicate by RP-HPLC (Agilent Technologies, Palo Alto, CA, USA) with UV−diode array absorption. The samples were eluted using a Lichrosphere C-18 (2.1 × 250 mm) column at 30 °C. The mobile phase was 70:30 (v/v) acetonitrile/water with 0.05% trifluoroacetic acid (TFA). The flow rate was 0.8 mL/min, and the detection wavelength was 320 nm. The concentration of FA standard (HPLC ≥ 98%; supplied by Shanghai Yuanye Biotechnology Co., Ltd., Shanghai, China) was 1 mg/mL, and the injection volume was 1 $\mu$L. All solvents were of HPLC grade and filtered through a 0.45 $\mu$m membrane. The FA content of samples was calculated from the peak area.[35]

**Determination of $T_2$ Relaxation Time by NMR.** The relaxation measurements were performed on a Niumag Desktop Pulsed NMR Analyzer (Shanghai Niumag Electronics Technology Co. Ltd.) with a magnetic field strength of 0.54 T and a corresponding resonance frequency for protons of 23.01 MHz. The NMR instrument was equipped with a 60 mm probe. Transverse relaxation ($T_2$) was measured using the Carr−Purcell−Meiboom−Gill (CPMG) pulse sequence, with a $\tau$ value (time between the 90° and 180° pulses) of 75 $\mu$s. Data from 2000 echoes were acquired as eight-scanned repetitions. The repetition time between two successive scans was 2 s. All relaxation measurements were performed at 25 °C. The $T_2$ relaxation time was analyzed by the distributed exponential fitting analysis using the Multi Exp Inv Analysis Software developed by Niumag Co., Ltd., China. A continuous exponentials distribution of the CPMG experiment was defined by eq 2

$$g_i = \int_0^\infty A(T)\, e^{-\tau_i/T}\, dT \tag{2}$$

where $g_i$ is the intensity of the decay at time $\tau_i$ and $A(T)$ is the amplitude of the component with transverse relaxation time $T$. Equation 2 was solved using Multi Exp Inv Analysis software by minimizing the function 3

$$\left(g_i - \int_{x=1}^{m} f_x\, e^{-\tau_i/T_x}\, dT\right)^2 + \lambda \sum_{x=1}^{m} f_x^2 \tag{3}$$

In formula 3, $\lambda$ is the weighting and $\lambda\sum_{x=1}^{m} f_x^2$ is a linear combination of functions added to the equation to perform a zero-order regularization.[36] The data were pruned from 2000 to 200 points using sampling pruning. This analysis resulted in a plot of relaxation amplitude for individual relaxation processes versus relaxation time. The time constant for each peak was calculated from the peak position, and the corresponding water contents were determined by cumulative integration. All calculations were measured using an in-house program written in combination of Matlab (Mathworks Inc., Natick, MA, USA) and Delphi (Borland, USA).

Three grams of bread dough prepared as described under Breadmaking was taken and placed into a test tube immediately after mixing. The water migration between AX gels and gluten in WWD systems with different particle size flours was observed using the NMR system that is represented by spin−spin relaxation times ($T_2$).

## RESULTS AND DISCUSSION

**Effects of WWF Granulation on Bread Volume and Specific Volume.** Generally, flour particle size that was measured by the laser particle size analyzer was a multipeak distribution. To obtain the average particle size of flour, the normal multipeak data were further processed with Origin software to fit a Gaussian distribution curve. The average particle sizes of the flour were the peak values of the fitted curves (Figure 1). The average particle sizes of three types of

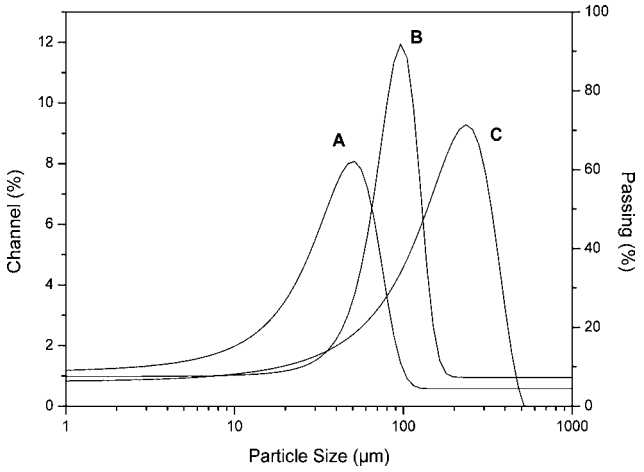


**Figure 1.** Fitted particle size distribution curves of whole wheat flour (WWF): (A) WWF with an average particle size of 50.21 $\mu$m, which was superfine ground by the ultramicro pulverizer for 15 min; (B) superfine ground for 25 min, average particle size of 96.99 $\mu$m; (C) superfine ground for 35 min, average particle size of 235.40 $\mu$m. The average particle size of the control flour (commercial flour) was 91.20 $\mu$m.

WWF from the milling experiment were 50.21 $\mu$m (A), 96.99 $\mu$m (B), and 235.40 $\mu$m (C), respectively. The average particle size of commercial bread flour (control) was 91.20 $\mu$m.

In the baking experiment, the effect of WWF of different particle sizes on baking quality was investigated. The results showed that the volume and specific volume of bread from WWF were lower than those of the white bread (Table 1). In addition, the WWB made from a medium particle size (96.99


dx.doi.org/10.1021/jf301195k | J. Agric. Food Chem. 2012, 60, 6507−6514

$\mu$m) WWF had larger volume and specific volume than those of the coarse (235.40 $\mu$m) or refined groups (50.21 $\mu$m).

**Table 1. Volume and Specific Volume of Whole Wheat Bread Baked from Whole Wheat Flour of Different Particle Sizes**[a]

| particle size ($\mu$m) | volume ($cm^3$) | weight (g) | specific volume ($cm^3$/g) |
|---|---|---|---|
| control[b] | 311.7 ± 16.1 a | 61.2 ± 1.8 a | 5.1 ± 0.2 a |
| 50.21 | 193.3 ± 7.6 c | 57.1 ± 0.8 c | 3.4 ± 0.2 c |
| 96.99 | 250.0 ± 13.2 b | 59.2 ± 0.6 b | 4.2 ± 0.2 b |
| 235.40 | 223.3 ± 5.8 b | 59.7 ± 2.0 b | 3.7 ± 0.1 b |

[a]Data are the mean value ± standard deviation. Values in the same column with the same letters are not significantly different ($P < 0.05$). [b]The control groups were made with commercial white flour. The average particle size of the control flour was 91.20 $\mu$m.

**Effect of WWF Granulation on the Porosity of WWB.** Three-layer scanned images (Figure 2) of WWB cross sections

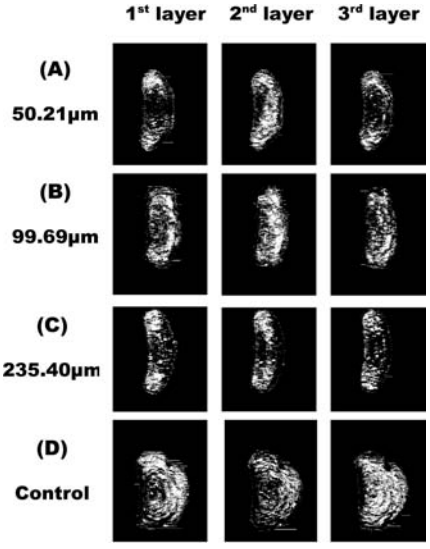


**Figure 2.** Weighted density of proton images scanned for three layers by the MRI system and processed using the threshold segmentation method: (A, B, C, D) scanned images of longitudinal sections of bread baked from whole wheat flour of particle sizes of 50.21, 96.99, 235.40, and 91.20 $\mu$m (control), respectively. The bright area of the scanned images is gas cells, and the dark part represents the bread skeleton.

were examined by the MRI system. The breads were baked from WWF of particle sizes of 50.21 $\mu$m (Figure 2A), 96.99 $\mu$m (Figure 2B), 235.40 $\mu$m (Figure 2C), and the control group (made from the commercial white flour) (Figure 2D), respectively. The bright areas of the images were gas cells, whereas the dark parts were bread skeleton. The greatest number and best distribution of gas cells were observed in the control group (Figure 2D) due to noninterference of wheat bran in the structure of the gluten network. Figure 2B shows more gas cells and better gas cell distribution than Figure 2A,C, especially on the second scanned layer, but slightly fewer than the control group. Although the differences of bright area between panels A and C of Figure 2 were not significant, the distribution of gas cells can still be observed. Also, the calculation of porosity can give secondary proof of the differences more precisely. The porosity (Table 2) calculated by the twice-threshold segmentation method also showed a similar trend. The breads made with WWF of particle size of 96.99 $\mu$m had a better crumb structure and baking performance than the other two WWF with larger or smaller bran particle sizes, but was second to the control group. The large particle wheat bran in WWF (235.40 $\mu$m) caused shearing and diluted the gluten matrix, inhibiting the formation of the gluten network and the structure and integrity of gas cells, which led to reduced gas retention by gluten protein membrane.[37] Thus, an uneven distribution of gas cells was formed during the releasing process of $CO_2$ gas in the early stage of baking. Small particles of wheat bran had a less destructive effect on the formation of the gluten network. However, Figure 2C also shows that the WWB with the smallest bran particle size had less porosity than the medium bran size group. To explain this phenomenon, we tentatively proposed that the dispersion of certain active compounds increased with the refinement of WWF particle size, especially the FA (a component of the AX gels), which has the ability to strengthen the AX gels.[38] Due to the better water sequestering capability of the AX gels than of the gluten matrix, the AX gels competed for water with the gluten network in WWD.[20] Thus, the formation of gluten was inhibited, because sufficient water for adequate protein hydration is a prerequisite for the development of gluten network. The quality of the gluten network determines the baking performance, so the fine particle size WWF (50.21 $\mu$m) led to less porosity than the medium particle size groups.

The competitive water sequestering between the AX gels and gluten network in the dough system was confirmed by the measurement of $T_2$ relaxation time using the MRI technique as detailed under Determination of T2 Relaxation Time by NMR.

**Effect of WWF Granulation on the Gluten Network.** Wheat bran can dilute and disrupt the gluten network, impair gas retention and bread texture and appearance,[7] and decrease the degree of softening and loaf volume.[39] Figure 3 shows various effects on the gluten network by wheat bran of various particle sizes: 50.21 $\mu$m (A), 96.99 $\mu$m (B), 235.40 $\mu$m (C), and 91.20 $\mu$m (control, D), respectively. In Figure 3A, a continuous and compact gluten network was observed resulting from the small particle size of the wheat bran. The continuous gluten matrix provided the precondition for superior baking quality, but an excessively compact gluten matrix was detrimental in obtaining good loaf volume.[40] In Figure 3B, the particle size of the bran was increased (indicated by the arrow), the shearing effect on the gluten matrix was increased, and the gas retention ability was weakened. In Figure 3C, the large particle size of wheat bran (indicated by the arrow) was present in the dough system; it sheared the gluten matrix significantly. The internal structure of the gluten network was fractured, discontinuous, and full of "clutter holes". During the fermentation and proofing stages of the baking process, the gas cells expand into an open network of pores.[41] The fragmented gluten network was unable to retain the $CO_2$ gas, and the gas was released in the early stages of breadmaking,[42] leading to small bread volume and inferior baking results.

**Effect of WWF Granulation on the Secondary Structures of Gluten Protein.** Seyer and Gelinas proposed that the deleterious effect on the gluten matrix of large wheat bran particles could be attributed to the breakage of secondary structure of gluten macropolymer during dough kneading.[43] To confirm this hypothesis, the dough system was investigated by FT-IR. The secondary structures of gluten protein (Table 3) are the $\alpha$-helix, $\beta$-sheet, $\beta$-turn, random coil, and $\beta$-antiparallel.

**Table 2. Calculation of the Porosity of Whole Wheat Bread Cross Section, Scanned by Magnetic Resonance Imaging, Processed Using the Threshold Segmentation Method[a]**

| particle size ($\mu$m) | scanned layers | threshold value 1 | $N_1$ | threshold value 2 | $N_2$ | porosity[b] (%) |
|---|---|---|---|---|---|---|
| control (91.20) | 1 | 30 | 134290 | 5 | 58218 | 37.74 ± 5.25 |
| | 2 | 40 | 128756 | 5 | 64332 | |
| | 3 | 40 | 128096 | 5 | 48364 | |
| 50.21 | 1 | 50 | 208517 | 10 | 37163 | 33.35 ± 9.32 |
| | 2 | 40 | 217024 | 10 | 56776 | |
| | 3 | 40 | 211807 | 10 | 36215 | |
| 96.99 | 1 | 50 | 123669 | 5 | 88162 | 38.21 ± 9.22 |
| | 2 | 50 | 136608 | 5 | 60010 | |
| | 3 | 50 | 125912 | 5 | 94685 | |
| 235.40 | 1 | 80 | 154704 | 80 | 43971 | 29.96 ± 5.08 |
| | 2 | 70 | 149476 | 50 | 39200 | |
| | 3 | 80 | 148623 | 80 | 32288 | |

[a]The pixels of twice threshold segmentation are represented by $N_1$ and $N_2$. Each bread sample was scanned for three layers. [b]Data are the mean value ± standard deviation.

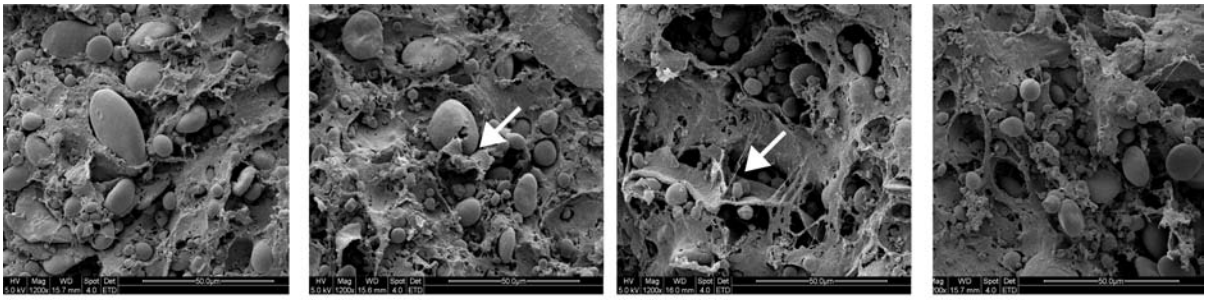


**Figure 3.** SEM images of whole wheat dough prepared with flour particle sizes of 50.21 $\mu$m (A), 96.99 $\mu$m (B), 235.40 $\mu$m (C), and 91.20 $\mu$m (control) (D), respectively. The arrows point to the wheat bran particles.

**Table 3. Content of Secondary Structure ($\alpha$-Helix, $\beta$-Sheet, $\beta$-Turn, Random Coil, and $\beta$-Antiparallel)[a] of Gluten Protein in Whole Wheat Dough Prepared with Flour of Different Particle Sizes**

| | peak frequency ($cm^{-1}$) | | | percentage[b] (%) | | |
|---|---|---|---|---|---|---|
| flour particle size: | 50.21 $\mu$m | 96.99 $\mu$m | 235.40 $\mu$m | 50.21 $\mu$m | 96.99 $\mu$m | 235.40 $\mu$m |
| $\alpha$-helix | 1655.8 | 1656.7 | 1657 | 26.74 ± 2.75 | 26.60 ± 2.03 | 24.08 ± 1.21 |
| $\beta$-sheet | 1617.2/1632 | 1617/1631.7 | 1617.1/1630.2 | 23.60 ± 2.66 | 23.18 ± 1.92 | 21.32 ± 1.07 |
| $\beta$-turn | 1668.9 | 1669.5 | 1668.2 | 19.21 ± 1.37 | 18.70 ± 1.46 | 17.19 ± 0.86 |
| random coil | 1644.5 | 1644.7 | 1648.6 | 20.10 ± 1.40 | 21.41 ± 2.05 | 28.14 ± 1.15 |
| $\beta$-antiparallel | 1681.5 | 1682 | 1681 | 10.35 ± 0.79 | 10.11 ± 0.89 | 9.27 ± 0.54 |

[a]The content of secondary structure of gluten protein was determined by FT-IR, represented by the percentage of peak area calculated from the fitted infrared spectrum. [b]Mean ± standard deviation (three replications).

**Table 4. Content of Ferulic Acid Determined by RP-HPLC in Whole Wheat Flour of Different Particle Sizes**

| | particle size[a] | | | |
|---|---|---|---|---|
| | 50.21 $\mu$m | 96.99 $\mu$m | 235.40 $\mu$m | standard sample |
| peak area | 6691.6 ± 6.4 | 2870.0 ± 5.7 | 1816.7 ± 4.4 | 7293.8 ± 0.5 |
| FA content (mg/mL) | 0.9200 ± 0.0010 | 0.3900 ± 0.0008 | 0.2500 ± 0.0006 | 1.00 |

[a]Mean ± standard deviation (three replications).

The content of $\alpha$-helix, $\beta$-sheet, $\beta$-turn, and $\beta$-antiparallel increased with the refinement of bran (reduction in particle size) contained in the WWF, while the content of random coil showed the opposite trend. Textural properties of gluten protein are mainly determined by the amount and balance of weak and strong physical linkages, hydrogen bond, hydrophobic interactions, electrostatic forces, covalent bonds, and disulfide bonds in dough system.[44] The secondary structures of gluten protein play an important role in forming the gluten network structure. Hydrogen bonds can be broken easily by

Table 5. $T_2$ Relaxation Time Distribution of Whole Wheat Dough of Different Flour Particle Sizes

| | particle size | | | | | | | | |
|---|---|---|---|---|---|---|---|---|---|
| | 50.21 μm | | | 96.99 μm | | | 235.40 μm | | |
| | $T_{21}$ | $T_{22}$ | $T_{23}$ | $T_{21}$ | $T_{22}$ | $T_{23}$ | $T_{21}$ | $T_{22}$ | $T_{23}$ |
| percentage | 0.0891 | 0.9042 | 0.0071 | 0.0563 | 0.9180 | 0.0123 | /[a] | 0.9880 | 0.0122 |
| SD[b] | 0.0011 | 0.0020 | 0.0005 | 0.0008 | 0.0020 | 0.0008 | / | 0.0030 | 0.0007 |

[a]/ indicates that no signal was detected. [b]SD, standard deviation.

Table 6. $T_2$ Relaxation Time Distribution of Whole Wheat Dough with Added Wheat Bran

| | bran addition | | | | | | | | | | | |
|---|---|---|---|---|---|---|---|---|---|---|---|---|
| | control[a] | | | 20% | | | 40% | | | 60% | | |
| | $T_{21}$ | $T_{22}$ | $T_{23}$ | $T_{21}$ | $T_{22}$ | $T_{23}$ | $T_{21}$ | $T_{22}$ | $T_{23}$ | $T_{21}$ | $T_{22}$ | $T_{23}$ |
| %[b] | /[c] | 0.9981 | 0.0020 | / | 0.9892 | 0.0111 | 0.0274 | 0.9590 | 0.0143 | 0.0293 | 0.9571 | 0.0142 |
| SD[d] | | 0.0028 | 0.0001 | | 0.0030 | 0.0002 | 0.0001 | 0.0022 | 0.0001 | 0.0006 | 0.0025 | 0.0001 |

[a]The control groups were made with commercial white flour. [b]Percentage of each peak area in total areas ($T_{21}$, $T_{22}$, and $T_{23}$). [c]/ indicates that no signal was detected. [d]SD, standard deviation.

wheat bran during kneading,[19] so the orderly secondary structures of proteins can be split into disordered structures like random coils. The higher content of α-helix, β-sheet, β-turn and β-antiparallel structures in the refined particle size of WWD, compared to the coarse group, suggested the conformation of gluten structure of refined particle size was more stable.[45] These results indicate that the large particle size of WWF, especially the wheat bran with hard texture, had more severe shearing effect on gluten proteins.

**Effect of WWF Granulation on the Content of Ferulic Acid.** To investigate the mechanism through which WWF of refined particle sizes had a destructive effect on the volume of bread, the content of FA (Table 4) was determined by RP-HPLC. Results showed that with the decreasing particle size of WWF, more FA was released from the wheat bran to participate in oxidative gelation. This can be attributed to the disruption of cells and the increased specific surface area of wheat bran.[37] Considering this theory, we confirmed that the strength of AX gels would increase with reducing particle size of WWF. This observation confirmed the hypothesis of competitive water sequestration between the AX gels and the gluten network, which verified that the bread made with refined particle size WWF had less porosity.

**Demonstration of Water Migration between AX Gels and Gluten by $T_2$ Relaxation Time.** To confirm that water migration and competitive water sequestration between the AX gels and gluten matrix were the primary causes for the inferior baking quality of WWF, the $T_2$ relaxation times of WWD with different particle size flours (Table 5) and wheat bran additions (Table 6) were examined by MRI.

The $T_2$ relaxation time graph includes three peaks: $T_{21}$ (0−1 ms), $T_{22}$ (1−100 ms), and $T_{23}$ (100−1000 ms), which represent bound water, immobilized water, and free water, respectively. The *X*-axis of the $T_2$ relaxation time represents the water activity in the food system. A longer $T_2$ relaxation time indicates a higher degree of water freedom. The *Y*-axis in the $T_2$ graph represents the signal amplitude of protons. The peak area of $T_2$ represents the relative content of hydrogen protons and the water absorption by hydrophilic components. The data (Table 5) show that the proportion of $T_{21}$ peak area percentage had a negative correlation ($r = -0.991$) with the decrease in particle size of the WWF. A positive correlation ($r = 0.996$) was found between the proportion of $T_{22}$ peak area percentage and the average particle size of WWF. There was no change in the peak area proportion of $T_{23}$. On the basis of the measurement of $T_2$ relaxation time from MRI, we inferred that the $T_{21}$ peak area may represent the amount of water bound by the esterified AX, essentially the cell wall material. The AX gels sequester water and make it unavailable to migrate freely,[46] but there is no effect on water activity (free water). These results implied that the content of FA that participated in an oxidative gelation reaction increased with the decrease in particle size of the WWF. The AX gel strength was reported to have a positive correlation with the content of FA;[35] therefore, as the particle size of the WWF decreases, the AX gels will be strengthened because of increased unesterified FA. In addition, AX gels contain many hydrophilic groups such as hydroxyl groups, which bond with water molecules through hydrogen bonds.[47] Although the porous structure of the gluten network also had strong water absorption ability,[48] the water retention ability of the gluten network is weaker than that of the AX gels, and the AX has much greater water-holding capacity than gluten proteins;[49] therefore, water tends to move from the gluten matrix to AX gels. It was hypothesized that the AX gels sequestered water, limiting the amount of water available to participate in gluten formation in the bread dough,[50] and the amount of AX gel influenced dough stickiness and water retention capacity.[51]

$T_{22}$ may represent the water trapped in the gluten network (immobilized water), which was the major existing form of water. $T_{23}$ may represent the free water distributed in the matrix between the AX gels and the gluten network in the WWD system. The amount of free water remained constant during the entire water migration process between the AX gels and the gluten network, which indicated that the amount of water lost from the gluten network was similar to the amount of the water obtained by the AX gels. This observation was in agreement with the fact that the AX gels only sequester water and do not affect water activity. This form of free water may be thought of as "water migration channels" between the AX gels and the gluten matrix.

The water sequestration competition mechanism between the AX gels and the gluten matrix, as well as the identification of each peak in the $T_2$ relaxation time experiment, was confirmed by the study of wheat bran addition (Table 6). The proportion of $T_{21}$ peak area percentage had a positive

correlation ($r$ = 0.888) with the increase in wheat bran addition in white flour dough (Table 6); a negative correlation ($r$ = −0.893) was shown in the proportion of $T_{22}$ peak area percentage. However, $T_{22}$ and $T_{23}$ had strong signals in dough systems that contained additional wheat bran. In the control group and the dough with 20% wheat bran added, no $T_{21}$ peak was detected due to its weak signal. When the addition of wheat bran was increased to 40%, $T_{21}$ signals were detected.

In conclusion, the water migration from the gluten network to AX gels as determined by the MRI technique confirmed that it was the main cause leading to the inferior baking quality of whole grain bread made with the refined particle size WWF.

## AUTHOR INFORMATION


### Corresponding Author

*(G.G.H.) E-mail: ghou@wmcinc.org. Phone: +1 (503) 295-0823. Fax: +1 (503) 295-2735. (Z.X.C.) E-mail: zxchen2007@126.com. Phone: +86 510-8587911. Fax: +86 510-85867273.


### Notes

The authors declare no competing financial interest.

## ACKNOWLEDGMENTS

We acknowledge Jin Lenong Agriculture Development Co., Ltd. (Henan Province, China), for providing the wheat sample and technical assistance by the Shanghai Niumag Electronics Technology Co., Ltd. (Shanghai, China).

## ABBREVIATIONS USED

AX, arabinoxylan; WWB, whole wheat bread; WWD, whole wheat dough; WWF, whole wheat flour; MRI, magnetic resonance imaging; FA, ferulic acid; AU, absorbance units; RP-HPLC, reversed-phase high-performance liquid chromatography; SEM, scanning electron microscope; FT-IR, Fourier transform infrared spectroscopy.

## REFERENCES


(1) Rosell, C. M.; Victor, R. P.; Ronald Ross, W.; Vinood, B. P. The science of doughs and bread quality. In *Flour and Breads and their Fortification in Health and Disease Prevention*; Academic Press: San Diego, CA, 2011; pp 3−14.

(2) Liu, R. H.; Okarter, N. Health benefits of whole grain phytochemicals. *Crit. Rev. Food Sci. Nutr.* **2010**, *50*, 193−208.

(3) Vitaglione, P.; Napolitano, A.; Fogliano, V. Cereal dietary fibre: a natural functional ingredient to deliver phenolic compounds into the gut. *Trends Food Sci Technol.* **2008**, *19*, 451−463.

(4) Schatzkin, A.; Park, Y.; Leitzmann, M. F.; Hollenbeck, A. R.; Cross, A. J. Prospective study of dietary fiber, whole grain foods, and small intestinal cancer. *Gastroenterology* **2008**, *135*, 1163−1167.

(5) Liu, R. H. Whole grain phytochemicals and health. *J. Cereal Sci.* **2007**, *46*, 207−219.

(6) Gelinas, P.; McKinnon, C. A finer screening of wheat cultivars based on comparison of the baking potential of whole-grain flour and white flour. *Int. J. Food Sci. Technol.* **2011**, *46*, 1137−1148.

(7) Jacobs, M. S.; Izydorczyk, M. S.; Preston, K. R.; Dexter, J. E. Evaluation of baking procedures for incorporation of barley roller milling fractions containing high levels of dietary fibre into bread. *J. Sci. Food Agric.* **2008**, *88*, 558−568.

(8) Yu, L.; Slavin, M. All natural whole-wheat functional foods for health promotion and disease prevention. In *Functional Food and Health. ACS Symp. Series* **2008**, *No. 993*, 125−142.

(9) Moore, Z. Wheat bran particle size effects on bread baking performance and quality. *J. Sci. Food Agric.* **1999**, *79*, 805−809.

(10) Salmenkallio-Marttila, M.; Katina, K.; Autio, K. Effects of bran fermentation on quality and microstructure of high-fiber wheat bread. *Cereal Chem.* **2001**, *78*, 429−435.

(11) Gan, Z.; Ellis, P. R.; Vaughan, J. G.; Galliard, T. Some effects of non-endosperm components of wheat and of added gluten on wholemeal bread microstructure. *J. Cereal Sci.* **1989**, *10*, 81−91.

(12) Moore, J. S. Shape-persistent molecular architectures of nanoscale dimension. *Acc. Chem. Res.* **1997**, *30*, 402−413.

(13) Gan, Z.; Galliard, T.; Ellis, P. R.; Angold, R. E.; Vaughan, J. G. Effect of the outer bran layers on the loaf volume of wheat bread. *J. Cereal Sci.* **1992**, *15*, 151−163.

(14) Moder, K. F.; Bruinsma, B. L.; Ponte, J. G. Bread-making potential of straight-grade and whole-wheat flours of Triumph and Eagle-Plainsman V hard red winter wheats. *Cereal Chem.* **1984**, *61*, 269−273.

(15) Piber, M.; Koehler, P. Identification of dehydroferulic acid-tyrosine in rye and wheat: evidence for a covalent cross-link between arabinoxylans and proteins. *J. Agric. Food Chem.* **2005**, *53*, 5276−5284.

(16) Fausch, H.; Kundig, W.; Neukom, H. Ferulic acid as a component of a glycoprotein from wheat flour. *Nature* **1963**, *199*, 287−287.

(17) Markwalder, H. U.; Neukom, H. Diferulic acid as a possible crosslink in hemicelluloses from wheat germ. *Phytochemistry* **1976**, *15*, 836−837.

(18) Wang, M. W.; Hamer, R. J.; Van Vliet, T.; Oudgenoeg, G. Interaction of water extractable pentosans with gluten protein: effect on dough properties and gluten quality. *J. Cereal Sci.* **2002**, *36*, 25−37.

(19) Autio, K. Effects of cell wall components on the functionality of wheat gluten. *Biotechnol. Adv.* **2006**, *24*, 633−635.

(20) Labat, E.; Rouau, X.; Morel, M. H. Effect of flour water-extractable pentosans on molecular associations in gluten during mixing. *Lebensm.-Wiss. -Technol. (Food Sci. Technol.)* **2002**, *35*, 185−189.

(21) Gill, S.; Vasanthan, T.; Ooraikul, B.; Rossnagel, B. Wheat bread quality as influenced by the substitution of waxy and regular barley flours in their native and extruded forms. *J. Cereal Sci.* **2002**, *36*, 219−237.

(22) Roman-Gutierrez, A. D.; Guilbert, S.; Cuq, B. Distribution of water between wheat flour components: a dynamic water vapour adsorption study. *J. Cereal Sci.* **2002**, *36*, 347−355.

(23) Stapley, A. G. F.; Hyde, T. M.; Gladden, L. F.; Fryer, P. J. NMR imaging of the wheat grain cooking process. *Int. J. Food Sci. Technol.* **1997**, *32*, 355−375.

(24) Hwang, S. S.; Cheng, Y. C.; Chang, C.; Lur, H. S.; Lin, T. T. Magnetic resonance imaging and analyses of tempering processes in rice kernels. *J. Cereal Sci.* **2009**, *50*, 36−42.

(25) Horigane, A. K.; Takahashi, H.; Maruyama, S.; Ohtsubo, K. i.; Yoshida, M. Water penetration into rice grains during soaking observed by gradient echo magnetic resonance imaging. *J. Cereal Sci.* **2006**, *44*, 307−316.

(26) Ghosh, P. K.; Jayas, D. S.; Gruwel, M. L. H.; White, N. D. G. A magnetic resonance imaging study of wheat drying kinetics. *Biosyst. Eng.* **2007**, *97*, 189−199.

(27) Shigehiro, N. I.; Hiroyuki, T.; Mika, K.; Hiromi, K. Routine evaluation of the grain structures of baked breads by MRI. *Food Sci. Technol. Res.* **2003**, *9*, 155−161.

(28) Sapirstein, H. D.; Roller, R.; Bushuk, W. Instrumental measurement of bread crumb grain by digital image analysis. *Cereal Chem.* **1994**, *71*, 383−391.

(29) Takano, H.; Ishida, N.; Koizumi, M.; Kano, H. Imaging of the fermentation process of bread dough and the grain structure of baked breads by magnetic resonance imaging. *J. Food Sci.* **2002**, *67*, 244−250.

(30) Naito, S.; Ishida, N.; Takano, H.; Koizumi, M.; Kano, H. Routine evaluation of the grain structures of baked breads by MRI. *Food Sci. Technol. Res.* **2003**, *9*, 155−161.

(31) Lodi, A.; Abduljalil, A. M.; Vodovotz, Y. Characterization of water distribution in bread during storage using magnetic resonance imaging. *Magn. Reson. Imaging* **2007**, *25*, 1449−1458.

(32) Ishida, N.; Takano, H.; Naito, S.; Isobe, S.; Uemura, K.; Haishi, T.; Kosse, K.; Koizumi, M.; Kano, H. Architecture of baked breads depicted by a magnetic resonance imaging. *Magn. Reson. Imaging* **2001**, *19*, 867−874.

(33) Brescia, M. A.; Sacco, D.; Sgaramella, A.; Pasqualone, A.; Simeone, R.; Peri, G.; Sacco, A. Characterisation of different typical Italian breads by means of traditional, spectroscopic and image analyses. *Food Chem.* **2007**, *104*, 429−438.
(34) Wellner, N.; Mills, C.; Brownsey, G.; Wilson, R. H.; Brown, N.; Freeman, J.; Halford, N. G.; Shewry, P. R.; Belton, P. S. Changes in protein secondary structure during gluten deformation studied by dynamic Fourier transform infrared spectroscopy. *Biomacromolecules* **2005**, *6*, 255−261.
(35) Wang, M. W.; Oudgenoeg, G.; van Vliet, T.; Hamer, R. J. Interaction of water unextractable solids with gluten protein: effect on dough properties and gluten quality. *J. Cereal Sci.* **2003**, *38*, 95−104.
(36) Teukolsky, S. A.; Vetterling, W. T.; Flannery, B. P. Modeling of data. In *Numerical Recipes in C: The Art of Scientific Computing*, 2nd ed.; Cambridge University Press: New York, 1992; Vol. 2, pp 656−706.
(37) Noort, M. W. J.; van Haaster, D.; Hemery, Y.; Schols, H. A.; Hamer, R. J. The effect of particle size of wheat bran fractions on bread quality − evidence for fibre-protein interactions. *J Cereal Sci.* **2010**, *52*, 59−64.
(38) Cura, D. E.; Lantto, R.; Lille, M.; Andberg, M.; Kruus, K.; Buchert, J. Laccase-aided protein modification: effects on the structural properties of acidified sodium caseinate gels. *Int. Dairy J.* **2009**, *19*, 737−745.
(39) Stojceska, V.; Ainsworth, P. The effect of different enzymes on the quality of high-fibre enriched brewer's spent grain breads. *Food Chem.* **2008**, *110*, 865−872.
(40) Gan, Z.; Angold, R. E.; Williams, M. R.; Ellis, P. R.; Vaughan, J. G.; Galliard, T. The microstructure and gas retention of bread dough. *J. Cereal Sci.* **1990**, *12*, 15−24.
(41) Salmenkallio-Marttila, M.; Autio, K. Light microscopic investigations of cereal grains, doughs and breads. *Lebensm.-Wiss. -Technol. (Food Sci. Technol.)* **2001**, *34*, 18−22.
(42) Campbell, G. M.; Herrero-Sanchez, R.; Payo-Rodriguez, R.; Merchan, M. L. Measurement of dynamic dough density and effect of surfactants and flour type on aeration during mixing and gas retention during proofing. *Cereal Chem.* **2001**, *78*, 272−277.
(43) Seyer, M.-E.; Gélinas, P. Bran characteristics and wheat performance in whole wheat bread. *Int. J. Food Sci. Technol.*; **2009**, *44*, 688−693.
(44) Selinheimo, E.; Autio, K.; Krijus, K.; Buchert, J. Elucidating the mechanism of laccase and tyrosinase in wheat bread making. *J. Agric. Food Chem.* **2007**, *55*, 6357−6365.
(45) Shewry, P. R.; Popineau, Y.; Lafiandra, D.; Belton, P. Wheat glutenin subunits and dough elasticity: findings of the EUROWHEAT project. *Trends Food Sci. Technol.* **2001**, *11*, 433−441.
(46) Elizabeth, C. M. Arabinoxylan gels: impact of the feruloylation degree on their structure and properties. *Biomacromolecules* **2005**, *6*, 309−317.
(47) Izydorczyk, M. S.; Biliaderis, C. G. Cereal arabinoxylans: advances in structure and physicochemical properties. *Carbohydr. Polym.* **1995**, *28*, 33−48.
(48) Izydorczyk, M. S.; Chornick, T. L.; Paulley, F. G.; Edwards, N. M.; Dexter, J. E. Physicochemical properties of hull-less barley fibre-rich fractions varying in particle size and their potential as functional ingredients in two-layer flat bread. *Food Chem.* **2008**, *108*, 561−570.
(49) Kweon, M.; Slade, L.; Levine, H. Solvent retention capacity (SRC) testing of wheat flour: principles and value in predicting flour functionality in different wheat-based food processes and in wheat breeding—a review. *Cereal Chem.* **2011**, *88*, 537−552.
(50) Day, L.; Augustin, M. A.; Batey, I. L.; Wrigley, C. W. Wheat-gluten uses and industry needs. *Trends Food Sci. Technol.* **2006**, *17*, 82−90.
(51) Bettge, A. D.; Morris, C. F. Oxidative gelation measurement and influence on soft wheat batter viscosity and end-use quality. *Cereal Chem.* **2007**, *84*, 237−242.